PAPER • OPEN ACCESS

Time-extended inductive tokamak discharges with differentially-tilted toroidal field coils

To cite this article: R. Gatto *et al* 2023 *Nucl. Fusion* **63** 046008

OPEN ACCESS
IOP Publishing | International Atomic Energy Agency
Nuclear Fusion
Nucl. Fusion **63** (2023) 046008 (12pp)
https://doi.org/10.1088/1741-4326/acb606

Time-extended inductive tokamak discharges with differentially-tilted toroidal field coils

R. Gatto[1,*], F. Bombarda[2], S. Gabriellini[1], S. Murgo[3] and V.K. Zotta[1]

[1] Department of Astronautical, Electrical and Energy Engineering, Sapienza University of Rome, Rome, Italy
[2] ENEA-FSN-FUSPHY, Frascati Research Center, Frascati, Italy
[3] Department of Industrial, Electronic and Mechanical Engineering, Roma Tre University, Rome, Italy

E-mail: renato.gatto@uniroma1.it

Received 14 October 2022, revised 8 January 2023
Accepted for publication 25 January 2023
Published 1 March 2023

Abstract

The strong toroidal magnetic field required for plasma confinement in tokamaks is generated by a set of D-shaped coils lying equidistant on meridian planes toroidally located around the central axis of the device. A major technological challenge tied to this configuration is represented by the large Lorentz force acting on the coils and arising from the interaction of the coils' currents with the magnetic field generated by the coil system itself. As this force is given by the cross product of the coil current and the magnetic field, various kinds of coil geometry modification have been proposed to alleviate this problem, from an inclination of the entire coil in order to maintain its planarity, to azimuthal tilting of all, or parts of, the coil profile. When the inner legs of the coils are tilted, apart from a reduction of the electromagnetic forces, a solenoid-like structure is formed which introduces additional magnetic flux linked to the plasma. Considering compact, high field devices, it is shown that when this additional flux is exploited, totally or in part, to ramp up the plasma current, the discharge time can be extended by a significant amount without resorting to noninductive current drive systems. Operational scenarios with inner-leg-tilted toroidal field coils are presented.

Keywords: magnetic fusion, tokamak, toroidal magnetic field coil, Lorentz force, poloidal magnetic flux, plasma current induction, operational plasma scenario

(Some figures may appear in colour only in the online journal)

1. Introduction

The large electromagnetic (EM), or Lorentz, forces acting on the toroidal field coils (TFCs) [1, 2], and the limited discharge time if the plasma current is generated inductively without resorting to (inefficient and expensive) noninductive drive mechanisms [3], are among the main scientific and technological challenges associated with the tokamak configuration for the magnetic confinement of thermonuclear plasmas.

The adoption of superconducting magnets, which has overcome the problem of coil heating during the discharge, has retained that of EM stresses [4], while introducing a new limit on the critical magnetic field that superconductors (in particular, low temperature ones) can sustain: the magnetic field on the axis in superconducting tokamaks is limited by its value at the inner toroidal field coil interface with the plasma. Even with superconducting coils, however, the time duration of the discharge is restricted by the amount of time-changing magnetic flux linked to the plasma, in short the 'volt-second (V-s)',

* Author to whom any correspondence should be addressed.

(a) *The complete magnet system of the modified tokamak device.*

(b) *Half-way cut of the tilted TFCs system.*

Figure 1. Rendering of the modified tokamak design considered in the study, with the inner legs of the D-shaped TFCs tilted in the azimuthal direction.

that the central solenoid (CS) can supply to induce the plasma current. The majority of the available flux is consumed by the ramp-up phase of the discharge to bring the plasma current to its nominal value. Afterwards, maintaining the plasma current during the flat-top phase requires a relatively small amount of V·s, especially in the presence of additional heating and a fusion burning core.

To address the first of these two problems (EM, or Lorentz, forces), various kinds of modification of the TFCs have been proposed, from an inclination of the meridian planes containing the coils, to a uniform, or differential, azimuthal tilting of part or even the entire profile of the coils [5–14]. In this paper, which is a continuation of the work presented in [13, 14], we consider TFCs with differential tilting (i.e. tilting angle changing along the coil's profile) restricted mainly to the inner region of the coil (high-field side), with the amount of tilting calculated with the objective of reducing the total EM forces acting on this region of the coil. In figure 1 we present a rendering of such a modified tokamak device for the simple case of inner legs of the TFCs tilted in the azimuthal direction by about 45°, and such to create a continuous electrical circuit. In figure 1(*a*), the conventional poloidal field (PF) coils system is shown with solid thick lines, and the location of the plasma is indicated by a central doughnut. The 'double-central solenoid' structure of the device is evident. The tilting of the coils permits an important reduction of the meridian EM forces acting on the coils [14], at the same time introducing additional out-of-plane force components (which add to those generated by the PF coils system and the plasma current), which are however of smaller magnitude with respect to the in-plane components. In principle, an opportunely tilted coil could lead to a simplification of the design due to the partial avoidance of structures devoted to supporting the EM loads.

The additional advantage stemming from the tilting of the TFCs is represented by the time-varying poloidal magnetic flux linked to the plasma created by a time changing toroidal field. Even though both the conventional CS and the new one associated with the coil tilting can provide a source of inductive flux for ohmic plasma current drive, an important difference is that the induction capability of the latter solenoid is intrinsically tied with toroidal magnetic field changes. Usually, the toroidal magnetic field is brought to its full value before the beginning of the plasma discharge and, in superconducting devices, is never switched off. However, if the off-pulse field is set to a lower value, then it can be raised to its nominal value during the plasma current start-up. With the tilted TFCs, the consequent time-varying flux linked to the plasma induces a loop voltage. Once the working value of the toroidal field is reached, the inductive action of the TFCs system terminates but, as shown in the present work, a synergic action of the two solenoids can increase by a significant amount the time duration of a totally inductive discharge. Indeed, if all of the plasma current, or a large part of it, can be generated while the current in the TFCs increases at the beginning of the discharge, then all or most of the V·s provided by the conventional CS can be employed to maintain the plasma current during the flat-top phase.

While, in principle, noninductive current drive systems are not required in the double-CS scenario just outlined, they might be needed in practice, but with reduced requirements with respect to the conventional tokamak scenario, both in assisting the current ramp-up, and extending even more the flat-top phase. Considering, in particular, the ramp-up phase, electron cyclotron heating is being considered for plasma start-up in ITER and DTT [15–17], on the basis of the experience being acquired these days on several machines [18–23], precisely with the purpose of saving precious V·s in the earliest phase of the discharge. In this context, the tilted TFCs can be considered a complementary tool for the same purpose.

The consequences of the tilting of part or even the entire profile of the TFCs on the EM forces has been extensively studied in a previous paper [14], using a Mathematica code specifically written for the purpose. The present work differs from [14] in two respects. First, we consider only one specific configuration characterized by a tilting restricted mainly to the inner leg of the TFCs, and we quantify the reduction of the EM forces due to the tilting using an upgraded version of the code. Second, we present a numerical study of operational scenarios in which the conventional CS and the new one generated by the tilting of the inner legs of the TFCs work together with the

goal of extending the duration of the plasma discharge without resorting to non-inductive means. To carry out our calculation we refer to the Ignitor device [24], because we have all the data required for the calculation, and also because this device represents the line of high-field, compact tokamaks, for which the limited time extension of the discharge is strongly related to the EM forces on the coils (and their heating), and to the amount of V·s that can be provided by a very compact CS.

The paper is organized as follows. The next section provides a review of the topic of EM forces acting on the TFCs of a tokamak device, and explains how the tilting of the coils can lead to a reduction of these forces. This section also presents the basic equations implemented in the numerical code specifically written to perform tilting optimization studies. Section 3 presents the reference device selected to perform the study, and describes the computational methodology adopted by the code to perform optimization studies, with emphasis on the upgrades with respect to the version used in [14]. A specific differentially-tilted coils configuration obtained with the goal of minimizing the total EM forces acting on the inner region of the coils is defined. Section 4 is devoted to the study of operational scenarios which could be envisaged when exploiting the magnetic flux generated by both the conventional CS and the one associated with the TFCs tilting. A summary and conclusion section ends the paper.

2. Reduction of the EM forces acting on conventional TFCs by coil differential tilting

Three sets of coils are required to magnetically confine a high-temperature plasma in a conventional tokamak device, (a) the toroidally symmetric TFCs system which encloses the plasma chamber, a 'doughnut' shaped metal vessel, (b) the CS housed in the bore of the doughnut, and (c) the external poloidal field coils (PF coils) system. The total current $I_{\rm tfc}$ flowing in the TFCs generates a toroidal field $B_{\rm t} = I_{\rm tfc}/5R$ (with field in T, current in MA, and radius in m) at the center location R inside the magnet cavity where the plasma vessel is located. The current swing of the CS induces a current $I_{\rm pl}$ in the plasma loop, which acts as the secondary 'single coil' of a transformer. This plasma current generates the PF $B_{\rm p}$, of weaker magnitude with respect to the toroidal component. The resulting field lines in the plasma region are helically wound around the torus, providing particle confinement. This magnetic configuration is however not sufficient to ensure plasma control: external PF coils are needed to provide the additional vertical field required for the stabilization, positioning and shape control of the plasma column. Note that in the conventional tokamak just described, no ideal coupling exists between the PF and the TF coils, or between the plasma and the TF coils, a fact that simplifies the EM calculation.

A major technological issue tied to the tokamak coils system just described resides in the large EM forces, of tens of MN, acting on the TFCs, and due to the interaction of the current flowing in the coils with the magnetic field they generate. The conducting plates of the coils experience in-plane (meridian) centrifugal forces that are highest on the inboard legs, where the toroidal field is strongest. If the field produced by the PF coils system and the plasma current is considered, an additional force component in the out-of-plane (azimuthal) direction is generated.

The problem of the EM forces on the TFCs is exacerbated in compact tokamaks aiming at producing large toroidal fields. For this reason, in the present paper, design parameters are adopted which are representative of these type of machines, even though the study applies, in principle, equally well to larger devices designed to operate with lower magnetic fields. With the recent progress in the field of high-temperature superconductor coils, compact high-field tokamaks have acquired a relevant role in magnetic fusion research, not only due to their economical advantage tied to their reduced size, but also for physics benefits such as an increased power density while maintaining good plasma stability properties [25, 26]. The necessity to support the large EM forces proper of high-field devices, however, complicates the design. For example, the compact, high field device ignitor has to implement several solutions to cope with the EM forces in the toroidal magnet: 'bucking' and 'wedging' between the TF and CS magnet coils, a preloaded structural steel shell (C-clamps) for mechanical compression, and an EM press.

As in [14], the issue of force reduction on the TFCs is addressed numerically using a Mathematica [27] code specifically written to find the local tilting angle of the TFCs profile which minimizes the total EM force (or a single component) acting on it. To evaluate the magnetic field produced by a toroidal coil, we approximate it by a single line conductor of infinitesimal thickness, therefore neglecting cross-sectional effects. The line conductor is then discretized into many short straight wires, each one producing a magnetic field according to the formula:

$$\mathbf{B} = \frac{\mu_0 I}{4\pi d}(\cos\theta_1 + \cos\theta_2)\hat{\boldsymbol{n}}\ , \tag{1}$$

where I is the current flowing in the wire, d is the distance between the wire and the observation point (where the magnetic field is calculated), θ_1 and θ_2 are the angles between the wire and the two lines connecting the two end-points of the wire to the observation point, and $\hat{\boldsymbol{n}}$ is the unit vector perpendicular to the plane containing the wire and the observation point, and pointing in the direction of the magnetic field. Note that the field provided by this formula is singular on the wire itself. To evaluate the field at the location of a selected wire, required to find the EM forces acting on it, we therefore superimpose the magnetic field produced by all wires except the one under consideration. The approximation introduced by this procedure is small, since the wires are short due to their large number (e.g. a single coil is discretized in a minimum of 64 straight wires, according to the sought accuracy).

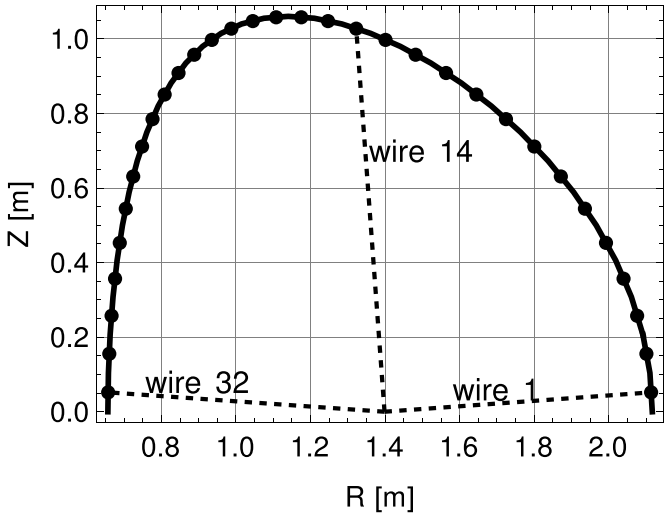

Figure 2. Center-points of wires in the case of a TFC discretized into 64 straight segments (symmetric region below the equatorial plane not shown).

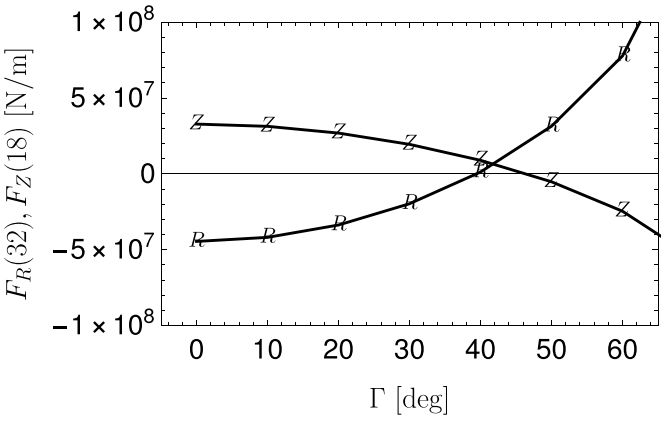

Figure 3. Radial (R) and vertical (Z) Lorentz forces (N m^{-1}) acting respectively on wire 32 ($\Theta \simeq 180$) and 18 ($\Theta \simeq 110$) of the toroidal field coils as the tilting angle Γ of all wires is increased from 0° to 60°. See figure 5 for a specification of the poloidal angle Θ.

To illustrate the calculation strategy, figure 2 indicates the locations of the center points of the wires, explicitly identifying three of them (wire n. 1, 14, 32, out of a total of 64 wires) drawing a dashed-line connecting their center-point with the central radial location of the coils. In the force reduction study, when a wire is tilted, its length is increased so to maintain the same Z coordinate of its end points. In this way, the tilted wire produces PF, while maintaining the same toroidal field as when the wire is non-tilted. In cylindrical coordinates, the expression of the Lorentz force acting on the unit length of the coil profile is given by

$$\mathbf{f} = \hat{\boldsymbol{R}}(I_\phi B_Z \underline{- I_Z B_\phi}) + \hat{\boldsymbol{\phi}}(I_Z B_R - I_R B_Z) + \hat{\boldsymbol{Z}}(\underline{I_R B_\phi} - I_\phi B_R)\ , \tag{2}$$

where $(\hat{\boldsymbol{R}}, \hat{\boldsymbol{\phi}}, \hat{\boldsymbol{Z}})$ are the coordinate versors, and the underlined terms indicate the force components acting on a conventional (non-tilted) coil. Considering the radial and vertical components, the additional (non-underlined) contributions are activated by the tilting of the coil, with a consequent reduction of the force. To show the change in the EM forces as the tilting angle is varied, the maximum radial and vertical force (which occur respectively at $\Theta = 180°$ and 110°, see figure 4, with Θ defined in figure 5) is computed as the tilting angle Γ in the azimuthal direction of *all* wires of the coil is increased from 0° to 60°. The results presented in figure 3 show the compensating action of the non-underlined terms in equation (2), leading to a reduction of the radial and vertical forces, the magnitude of which approaches zero around $\Gamma \sim 40°$ of tilting.

Equations (1) and (2) are the expressions implemented in the code to evaluate the EM forces. The code allows us to compute the optimal tilting angle in the azimuthal direction with the goal of minimizing the modulus of the force acting on a wire, or one or more selected components of the force. The optimization procedure is iterative, in the sense that all wires in the upper plane ($Z > 0$—all our studies consider configurations with up-down symmetry) are optimized in sequence, until convergence.

3. Calculation of the TF coils system with tilted inner region for Lorentz force reduction

To conduct our study, we consider a tokamak device with TFCs centered at $R_c = 1.39$ m, with the shape of the coils characterized by nominal values of the ellipticity and triangularity equal to, respectively, $\kappa_c = 1.44$ and $\delta_c = 0.344$. The toroidal magnetic field on axis has a strength of 13 T, and the plasma current at flat-top is equal to 11 MA. These parameters are proper of the Ignitor project, but well represent other proposals of compact high-field tokamaks such as SPARC [28]. The PF coils system is also derived from the Ignitor design. We choose to refer to the Ignitor parameters mainly because we have at our disposal all the data characterizing a standard operational scenario, which can then be used as a reference point for our study. Moreover, the choice is appropriate because in this type of device (compact, high field) the problem of the EM forces on the coils and of the limited time-extension of the discharge is exacerbated. In figure 4 we present the EM forces per unit length acting on the profile of a conventional (i.e. not tilted) D-shaped TFC, as a function of the poloidal angle. The greatest magnitude is found in the radial component (44.55 MN m^{-1}), and is localized in the inner region of the coil, while the vertical component reaches its maximum value in the upper (and symmetrically lower) coil region.

In [14], the effect on the EM forces of several tilted TF coils configurations have been investigated, including configurations with tilting extended to the entire profile of the coils. In the present work, the focus is on one specific case of differentially tilted TFC, the one obtained by tilting mainly its inner region with the goal of reducing the total force per unit length (a rendering of this configuration has been shown in

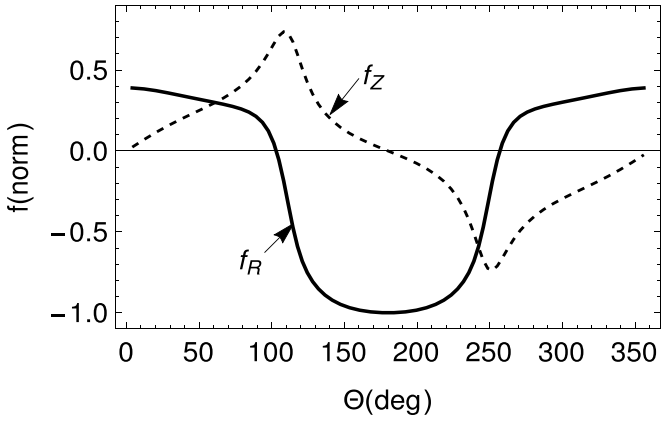

Figure 4. Radial and vertical forces (normalized to 44.55 MN m^{-1}) acting on the toroidal field coil of the reference configuration. The poloidal angle is counted from the equatorial plane on the low-field side of the coil.

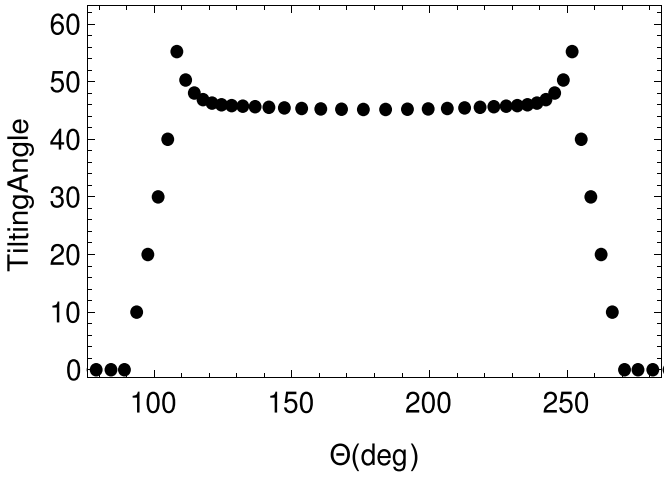

Figure 6. Optimal tilting angles (the numerical values are also reported in table 1 of section 4.2).

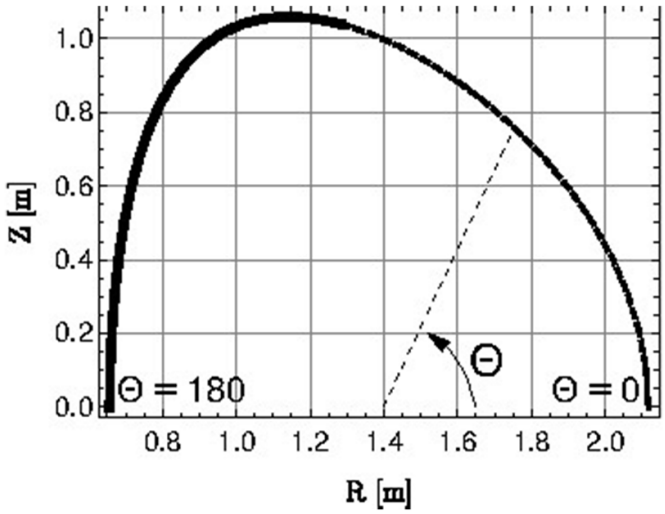

Figure 5. Region of tilting (thick line) in the optimization study, going from $\Theta \sim 93°$ to $\Theta \sim 180°$ (symmetric region below the equatorial plane not shown).

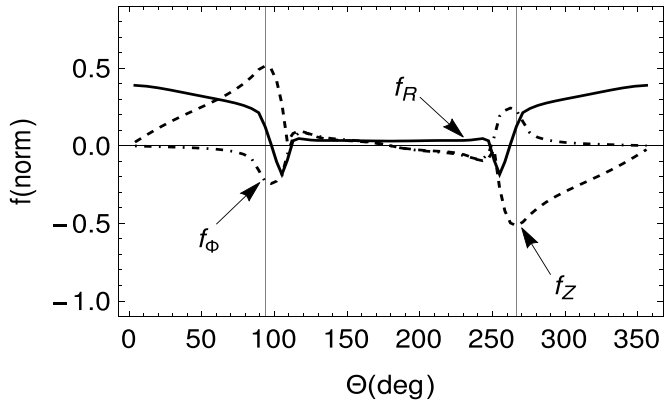

Figure 7. Radial and vertical forces, normalized to 44.55 (MN m^{-1}), acting on the toroidal field coil of the tilted configuration.

figure 1). The region of tilting, shown with a thick continuous line in figure 5, comprises wires 14–32 (and wires symmetric with respect to the equatorial plane). Note that also part of the upper region of the coil is tilted because the vertical forces are largest there. In the optimization procedure, the wires are free to be tilted up to a maximum angle of 60°, except for wires 14, 15, 16 and 17 (refer again to figure 2) whose maximum tilting angle is reduced to 10°, 20°, 30° and 40°, respectively, in order to produce a smooth transition between the nontilted and tilted region of the coil.

The tilting angles resulting from this optimization study, about 45° near the equatorial plane, are shown in figure 6, while figure 7 presents the radial, vertical and azimuthal components of the normalized force as a function of the poloidal location along the coil profile. The computed force is due only to the magnetic field produced by the TFCs system, as the contributions from the plasma current and the equilibrium PF coils are not included in the calculation. Comparing with figure 4, it is seen that both the radial and the vertical components are notably reduced in the region of tilting. The out-of-plane (azimuthal) component, introduced by the tilting, is of smaller magnitude: For example, the ratio of the maximum value of the azimuthal and vertical components, occurring at the boundary between the tilted and non-tilted region of the coil, is equal to 0.47. As in the conventional case of planar TFCs, in which this component of the EM force is due to the magnetic field produced by coils other than the TFCs as well as the plasma current, coping with this force component is easier due to the adjacency of the TFCs in the azimuthal direction.

The code used in the present work is an upgraded version of the one used in [14], in that it is now able to pass from an optimized but segmented TF coil to a continuous coil, and then connect all coils to end up with a TF coils system consisting of a continuous electrical circuit. This upgrade is now illustrated. At the end of the optimization procedure, in

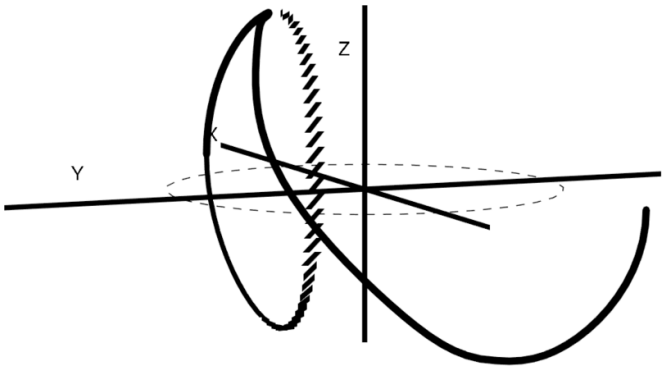

Figure 8. A single segmented (planar) coil obtained by the optimization calculation, and the corresponding continuous coil extending in the azimuthal direction.

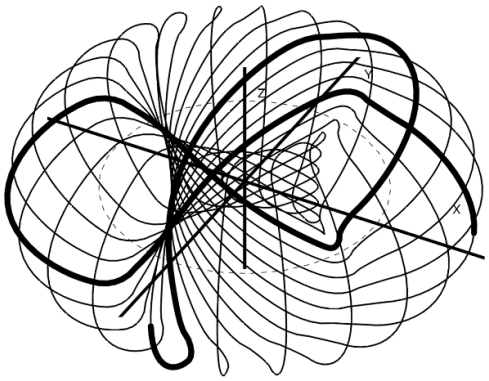

Figure 9. The optimized TF coils system constituted by a continuous electrical circuit.

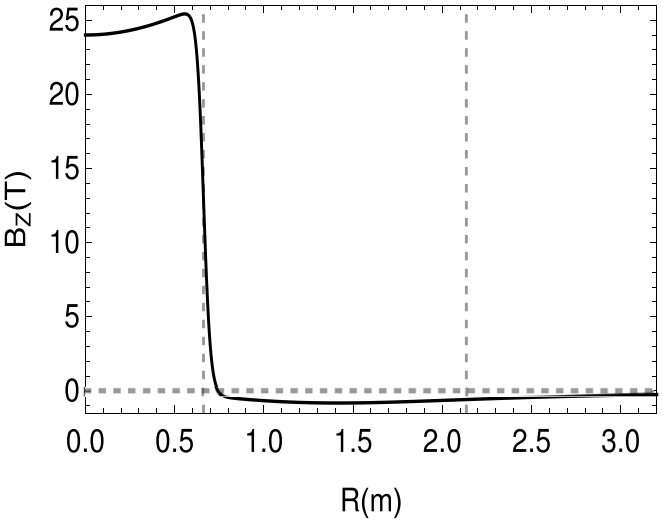

Figure 10. Major radius dependence of the vertical field produced by the tilted TFCs system. The dashed vertical gridlines indicate the inner and outer radii of the TFCs. The horizontal gridline indicates the $B_Z = 0$ value.

which each wire is tilted around its fixed center-point, the code reconstructs the continuous version of the coil by translating in the azimuthal direction each tilted wire. The procedure is illustrated for a single coil in figure 8. Since the tilting angles have been calculated with the only goal of minimizing the Lorentz forces, when the 24 TFCs are assembled together they do not form in general a continuous electrical circuit. An ad hoc subroutine which generates a continuous circuit has therefore being created. This subroutine changes (increasing or decreasing) the tilting angles of all coils' wires by the minimum amount necessary to close the circuit. For our configuration, it has been found that the required change of the tilting angle amounts to only 0.8% relative to the initial value. As a consequence of this change, the forces are not anymore minimized. Due to the very small change of the tilting angles, however, the increase in the EM forces is small. This force increase can be accepted if having a TF coils system made of a continuous electrical circuit turns out to be more convenient from an engineering point of view. The final TFCs system is shown in figure 9, where three connected coils have been put in evidence with a thicker line to better show the continuity of the system.

To verify that the tilting does not change the toroidal field, and that the optimized TFCs systems with segmented and continuous coils produce the same field, we have calculated the toroidal and vertical field at $(R,Z) = (R_0, 0)$, R_0 being the major radius, produced by the nontilted TFCs system, the segmented optimized TFCs system, and the continuous optimized TFCs system, finding respectively, $(B_\phi, B_Z) = (-13.00, 0)$, $(-13.00, -0.80)$, and $(-13.00, -0.81)$. The toroidal field values are equal, while the difference in the vertical fields (created by the tilting of the upper region of the coils) is less than 1.2%, so that an iterative procedure aiming at the convergence between the magnetic field produced by the two TFCs systems (segmented and continuous) is therefore not required, at least to the level of accuracy sought in this work. In figure 10, the radial variation of the vertical magnetic field produced by the optimized TFCs system is reported. The maximum value of the vertical magnetic field inside the TF chamber is 0.81 T, a small value for a high field device, and it is directed in the negative Z direction. When crossed with the plasma current, it leads to an outward force (in the $+R$ direction). A dedicated PFC should compensate this field to ensure plasma toroidal force balance. Moreover, since the field produced by this dedicated coil would add to the one produced by the tilted TFCs in the region $[0, R_{\rm in}^{\rm tfc}]$ where $R_{\rm in}^{\rm tfc} = 0.662$ m is the radial location of the TFCs inner legs, this coil would contribute to plasma current induction during the startup phase of the discharge.

We end this section by pointing out that the tilting optimization could be activated on a different region of the coil profile, and/or it could be pursued with a goal different from the minimization of the total force, as we did. As an example of the latter situation, consider the case of a compact high-field device in which the inner legs of the TFCs 'buck' against the CS so to obtain a compensation between the radial forces acting on the CS (outward) and on the TFCs (inward). From figure 7 we see that the radial force acting on the equatorial location of the TFC inner leg, even though it is nonzero, is much

reduced by the tilting (numerically, we obtain an optimized force of 1.37 MN m^{-1}, to be compared with the nontilted case of 44.55 MN m^{-1}). This means that even though the 'bucking' effect is not totally lost, it is notably reduced, and this could be a negative consequences of the tilting (which goes alongside to the beneficial effect of the drastic reduction of the vertical force). This 'weakening' of the bucking effect might require some engineering solution which makes the CS more apt to withstand the radial expansion forces or, alternatively, it might be convenient to optimize the tilting of the TFCs not to obtain the minimum possible radial force, but to maintain a certain amount of it for bucking purposes. For example, looking at figure 3 we see that the maximum radial and vertical forces are never zero together, the radial component vanishing at about 40°, while the vertical at about 46°. An optimal tilting with the goal of minimizing the vertical component and at the same time leaving a residual component of the radial component for 'bucking' purposes should then be possible.

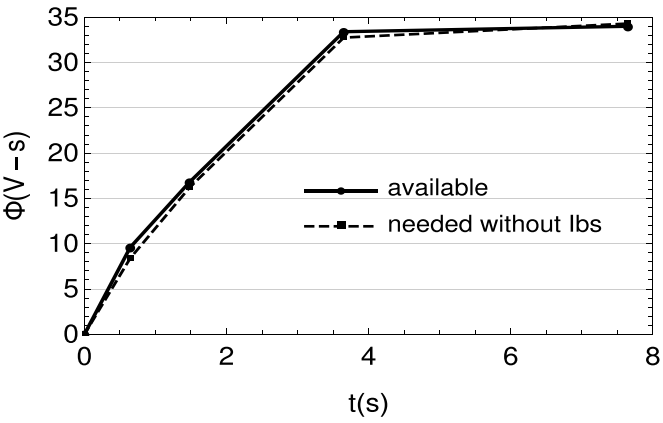

Figure 11. Time evolution of the magnetic flux (the available one, and the one needed without considering the bootstrap current contribution) for the 13 T–11 MA Ignitor scenario presented in [30] (only part of the original figure has been reproduced to adapt to the scope of the present paper).

4. Time-extended discharges

To date, the suggestion of tilting part of, or the entire, profile of the TFCs has been put forward in the literature, mainly stressing the beneficial consequence of reduced EM forces. Little attention has been posed on the impact on the discharge evolution of the additional poloidal flux linked to the plasma generated by the tilted TFCs system [5, 6, 29]. This latter effect, however, may turn to be, in our opinion, an advantage at least of the same relevance of that of force reduction. This additional flux linkage can indeed be used to partially or even totally ramp-up the plasma current, leaving to the conventional CS the only task of maintaining it. The synergic action of the conventional CS and the additional one due to TFCs tilting can in principle lead to plasma discharges of much longer duration.

A crude estimate on how long the conventional CS can maintain the flat-top plasma current, assuming that the ramp-up phase has been accomplished using the solenoid associated with the tilted TFCs, can be obtained by considering the V·s time evolution reported in [30], and represented graphically in figure 11. The values of the curve describing the flux needed without considering the bootstrap current contribution (dashed curve) at the beginning ($t = 3.65$ s) and end ($t = 7.65$ s) of the 4 s flat-top phase of the Ignitor scenario under consideration are 32.80 and 34.25 V·s, so that the flat-top plasma current sustenance requires a change of 1.45 V·s. Being the total available CS flux for the discharge equal to 34 V·s, and assuming that it is used only for maintaining the flat-top plasma current, we estimate that the flat-top can be extended by a factor of ∼23.

To improve on this crude estimate, a simulation of the entire evolution of the plasma discharge should be carried out using a 1.5 D transport code coupled with an equilibrium solver (e.g. the JETTO code [31]), opportunely modified to include the tilting of the TFCs. In the present work, we limit our self to a less demanding task, that is, we investigate the potentiality to time-extend a tokamak discharge with a tilted TFCs system by numerically solving, adopting a fourth order Runge–Kutta algorithm, the following circuital model for the time evolution of the plasma current:

$$L(t)\frac{\mathrm{d}I_{\mathrm{pl}}(t)}{\mathrm{d}t} + R_{\mathrm{res}}(t)I_{\mathrm{pl}}(t) = -\sum_{j}^{N_{\mathrm{cs}}} M_{\text{cs-pfc,j}}(t)\frac{\mathrm{d}I_{\text{cs-pfc,j}}(t)}{\mathrm{d}t} - \sum_{j}^{N_{\mathrm{eq}}} M_{\text{eq-pfc,j}}(t)\frac{\mathrm{d}I_{\text{eq-pfc,j}}(t)}{\mathrm{d}t} - \sum_{j}^{\bar{N}_{\mathrm{tfc}}} M_{\text{cs-tfc,j}}(t)\frac{\mathrm{d}I_{\text{cs-tfc,j}}(t)}{\mathrm{d}t}\,, \quad (3)$$

where I_{pl} is the plasma current, L is the total plasma inductance, R_{res} is the plasma resistance, $M_{\text{cs-pfc}}, M_{\text{eq-pfc}}, M_{\text{cs-tfc}}$ are respectively the mutual inductances between the plasma and the conventional CS (N_{cs} in number), the equilibrium PF coils (N_{eq} in number), and the CS associated with the tilting of the TF coils ($\bar{N}_{\mathrm{tfc}}$ will be defined in section 4.2), and $I_{\text{cs-pfc}}, I_{\text{eq-pfc}}, I_{\text{cs-tfc}}$ are the corresponding coils' currents. No contribution from bootstrap current or noninductive current drive has been included in the model.

Equation (3) governs the time evolution of the total plasma current, given as inputs the time evolution of the currents flowing in the coils, and includes the contribution from the tilted TFCs (last term on the RHS). The internal and mutual inductances and the plasma resistance are evaluated at each time step of the numerical calculation as follows. Adopting for simplicity cylindrical geometry, the plasma current profile is modeled as $J_{\mathrm{pl}}(r,t) = J_0(t)[1-(r/a(t))^{m_J(t)}]^{\nu_J(t)}$, where $a(t)$ is the plasma minor radius, the time evolution of which during the ramp-up phase is given, and the values of the time-varying coefficients m_J and ν_J are such to reproduce the results

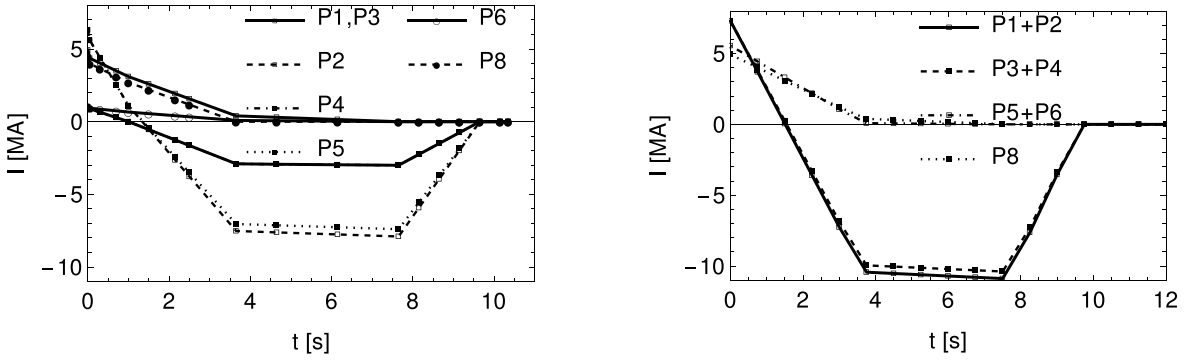

(a) *CS coils' currents as in Ref.[32].* (b) *CS coils' currents adopted in our numerical simulation.*

Figure 12. Time evolution of the currents in the CS coils above the equatorial plane.

obtained in the more accurate numerical modeling of [32], as described in section 4.1. From the plasma current density profile we calculate the poloidal magnetic field $B_{\mathrm{pl},\theta}(r,t)$, and then the internal inductance according to the formula ([33, p 281])

$$L_{\mathrm{int}}(t) = \frac{8\pi^2 R_0}{I_{\mathrm{pl}}^2(t)} \int_0^{a(t)} \frac{B_{\mathrm{pl},\theta}(r,t)}{2\mu_0} r\mathrm{d}r \,,$$

where R_0 is the major radius. For the external plasma inductance we use the formulation presented in [34],

$$L_{\mathrm{ext}}(t) = \mu_0 R_0 \frac{f_1[\varepsilon(t)]\,[1-\varepsilon(t)]}{1-\varepsilon(t)+f_2[\varepsilon(t)]\kappa} \,,$$

where $\varepsilon(t) = a(t)/R_0$ is the inverse aspect-ratio, κ is the plasma ellipticity, and we have introduced the two functions $f_1[\varepsilon(t)] = [1+1.81\varepsilon(t)^{1/2}+2.05\varepsilon(t)]\ln[8\varepsilon(t)^{-1}] - [2+9.25\varepsilon(t)^{1/2}-1.21\varepsilon(t)]$ and $f_2[\varepsilon(t)] = 0.73\varepsilon(t)^{1/2}[1+2\varepsilon(t)^4-6\varepsilon(t)^5+3.7\varepsilon(t)^6]$. The mutual inductance between plasma and the various set of coils are calculated from their defining relation, $M = \Phi_{\mathrm{B}}/I_{\mathrm{c}}$ where Φ_{B} is the flux linked with the plasma and I_{c} the current in the coils creating the flux. Finally, the plasma resistance is evaluated as $R_{\mathrm{res}} = (\int_V \eta J_{\mathrm{pl}}^2 \mathrm{d}V)/I_{\mathrm{pl}}^2$, where the integration is over the plasma volume, and the plasma resistivity is given by ([33, p 240])

$$\eta(t) = \frac{m_e^{1/2} e^2 \ln\Lambda}{2^{1/2} 6\pi^{3/2}\epsilon_0^2} \frac{F(Z_{\mathrm{eff}})}{T_e(t)^{3/2}} \,,$$

with $F(Z_{\mathrm{eff}}) = (1+1.198Z_{\mathrm{eff}}+0.222Z_{\mathrm{eff}}^2)/(1+2.966Z_{\mathrm{eff}}+0.753Z_{\mathrm{eff}}^2)$. In our calculation we have assumed an effective atomic number of the plasma equal to $Z_{\mathrm{eff}} = 1.20$.

The code considers a radial profile not only for the plasma current density but also for the plasma density and temperature (in particular $n, T \propto [1-(r/a)^\alpha]^\beta$ with $\alpha = 2, \beta = 1.5$), and introduces in all formulas the volume average for n, and the volume density-average value for T. For this reason, we refer to our code as a 0.5D code.

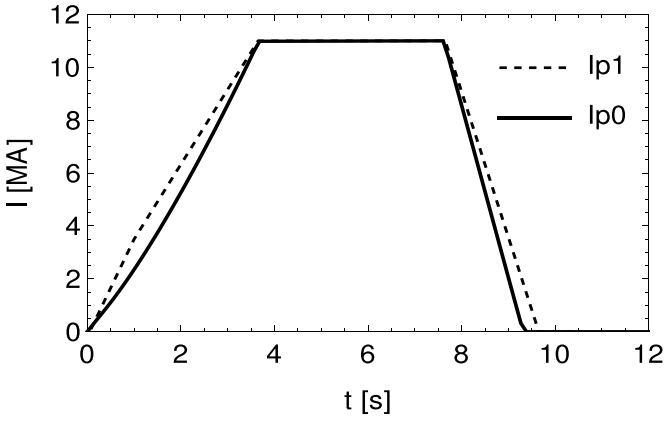

Figure 13. Time evolution of the plasma current. Ip1 is the is the 'real' time evolution as computed in [32], while Ip0 is the results of our numerical solution of equation (3).

4.1. Reference discharge with conventional TFCs

Before addressing plasma discharges with a tilted TFCs system, the code based on equation (3) has been 'calibrated' against an 11 MA–13 T plasma scenario studied in the context of the Ignitor program [32].

A comparison between the 'real' results (that is, those obtained in [32] with a more advanced numerical approach based on a 1.5D transport code coupled with a Grad–Shafranov equilibrium solver) and the output from our 0.5D code solving equation (3) is presented in figures 12 and 13. Figure 12(*a*) presents the time evolution of the currents flowing in the CS coils according to [32]. The Ignitor design foresees seven pairs of CS coils (each pair fed by a dedicated power supply, constituting a coil located above the machine equatorial plane, and one symmetrically below) named P1, P2, P3, P4, P5, P6 and P8. In our simulation we reduce the number of CS coils to four pairs, unifying the coils located at the same vertical location (P1 and P2, P3 and P4, P5 and P6, P8), positioning them at the radial center point of the outermost coil (that is, coil P2, P4, P6 and P8). The currents flowing in these coils are presented in figure 12(*b*). The comparison of the time evolution of the plasma currents induced by the CS

coils of figures 12(*a*) and (*b*) is presented in figure 13. The plasma current reaches its maximum value at 3.65 s, and it begins its ramp-down at 7.65 s, defining a flat-top of 4 s. The figure shows that, despite the many approximations characterizing our approach, including the facts that the time-evolution of the central values of the temperature and density have been modeled with simple trapezoidal functions (linear increase, horizontal flat-top line, and linear decrease), that the number of PF coils has been halved, that we are neglecting all coil–coil mutual interactions, and that our 0.5D model cannot reproduce the exact evolution of the plasma profiles, the result obtained with our code can be considered satisfactory, and suitable for the comparative study between conventional and tilted TFCs configuration that we are planning to perform. The 'calibration' leading to this result has been obtained by appropriately changing during the discharge the 'peakness' parameter $\nu_J(t)$ entering the current density profile. The operational scenario just presented is representative of conventional ohmic tokamaks, with both ramp-up and flat-top phases driven by the CS, the latter phase being necessarily of limited time extension.

4.2. Time-extended scenarios with tilted TFCs

In the selected reference device, a 13 T toroidal magnetic field is generated at flat-top by flowing in each of the 24 TFCs a current equal to $I_{\rm tfc} = 3.57$ MA [32]. The tilting of the wires in the inner region of the TFCs introduces an azimuthal component of the TFC current proportional to the degree of tilting; when time-changing, this current creates a poloidal flux linked to the plasma which induces a loop voltage. To represent this effect, modeled by the last term in equation (3), we have introduced additional circular 'CS coils' equal in number to the number of tilted wires of one TFC (indicated by $\overline{N}_{\rm tfc}$), with each circular coil passing through the center-point of the corresponding tilted wire. The current flowing in each one of these additional circular coils 'j' ($j = 1, \ldots, \overline{N}_{\rm tfc}$) is written as $I_{\text{cs-tfc,j}}(t) = [I_{\rm tfc}(t)\sin(\Gamma_j)] \times \overline{\alpha}_{\rm tfc}$, where Γ_j is the tilting angle of coil j (that is, of the associated wire, with tilting in the $+\phi$ direction). The constant factor $\overline{\alpha}_{\rm tfc}$ is introduced to take care of the fact that the projection in the azimuthal direction of the tilted wires of the 24 TFCs does not generate a continuous circular coil. This factor is found as follows. With the optimization code used to carry out the studies presented in section 3 we have evaluated the poloidal flux created by the tilted inner regions of the TFCs at flat-top: $\Phi_{\rm B,tfc} = 32.52$ V·s. The factor $\overline{\alpha}_{\rm tfc}$ is then found using an iterative procedure which imposes the equality of $\Phi_{\rm B,tfc}$ with the flux created by the $\overline{N}_{\rm tfc}$ circular coils. In figure 14 we show the system of coils modeled by equation (3) to simulate time-extended scenarios. The radius of the first circular coil of the conventional CS located above the equatorial plane, and of the one associated with the tilting of the TFCs are, respectively, equal to 0.510 and 0.663 m. Table 1 reports the tilting angles of the coil wires (presented graphically in figure 6), and the maximum currents (at flat-top) flowing in the circular coils mocking up the TFCs tilting. Considering this optimized tilting configuration, two operational scenarios (denoted Scenario A and Scenario B) are presented next, comparing them with the conventional discharge of section 4.1.

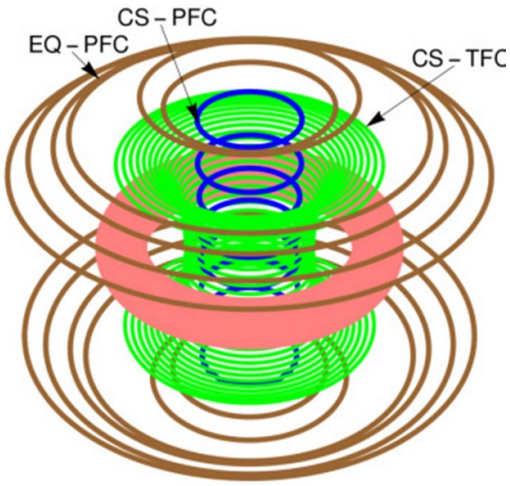

Figure 14. System of coils modeled by equation (3) when studying time extended discharges. From the central device axis outward: the conventional CS (CS-PFC) shown in dotted line-style, the additional CS generated by the tilting of the TFCs (CS-TFC), and the equilibrium coils (EQ-PFC). The additional thick doughnut indicates the plasma location.

Table 1. Tilting angles and maximum currents of the circular coils making up the CS associated with the tilting of the TFCs, as obtained by the procedure outlined at the beginning of section 4.2. Circular coils $1, 2, \ldots, 19$ correspond to tilted wire $32, 31, \ldots, 14$ in figure 2. Data relative to the coil profile below the equatorial plane are not reported.

CS-TFC	Γ (°)	$I_{\text{cs-tfc}}$ (MA)
1	45.55	1.359
2	45.60	1.360
3	45.65	1.361
4	45.72	1.363
5	45.83	1.365
6	45.93	1.367
7	46.04	1.370
8	46.13	1.372
9	46.22	1.374
10	46.37	1.378
11	46.67	1.384
12	47.27	1.398
13	48.43	1.424
14	50.71	1.473
15	55.68	1.572
16	40.34	1.232
17	30.25	0.959
18	20.17	0.656
19	10.08	0.333

4.2.1. Scenario A. Scenario A is based on the idea of exploiting the current rise in the TFCs to ramp up as much as possible the plasma current, which is then maintained during the flat-top phase using the conventional CS. The output of this study will be a theoretical upper bound on the maximum

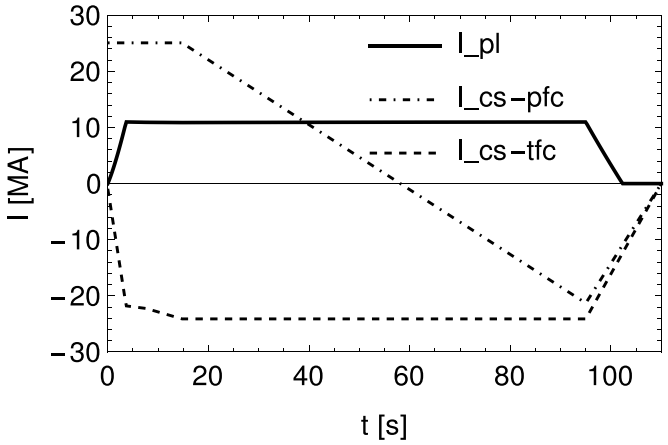

Figure 15. Extended operative scenario A.

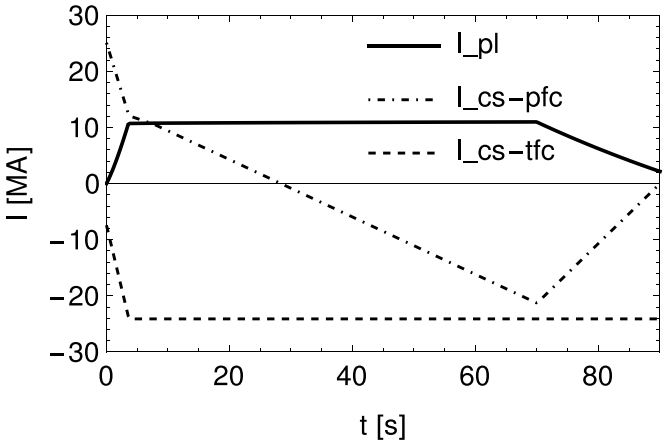

Figure 16. Extended operative scenario B.

discharge duration when both solenoids are employed. When analyzing this scenario, it has been found that the poloidal flux-swing generated by the CS associated with the TFCs tilting (we refer to the latter with the acronym 'CS-TFC'), (plus the one due to the equilibrium coils (we refer to the latter with 'EQ-PFCs')) is more than sufficient to ramp up the plasma current to its nominal value, totally dispensing the conventional CS from contributing to this initial phase of the discharge. Therefore, after the plasma current has reached its maximum value, its sustenance is achieved initially by the residual increase of the TFC's current, and then, after the nominal value of the toroidal field is reached, by the action of the conventional CS. It is worth noting that the direction of the current flowing in the TFCs is not arbitrary, as it is in a conventional tokamak, and its verse must be chosen so as to drive the plasma current in the same direction as the conventional CS does. In particular, in our simulations we have chosen the $-\phi$ and the $+\phi$ directions for the current flowing at flat-top in the conventional CS (we refer to the latter with 'CS-PFC') and CS-TFC circuits shown in figure 14. The results of the modeling of this scenario are presented in figure 15, which shows the time-evolution of the total plasma current, $I_{\rm pl}$, the total current flowing respectively in the conventional CS, $I_{\rm cs\text{-}pfc}$, and in the CS generated by the TFCs tilting, $I_{\rm cs\text{-}tfc}$ (considering only the coils above the equatorial plane). In the first phase of the discharge ($0-3.65$ s) the plasma current is ramped up to its maximum value of 11 MA by increasing the current in the TFCs so as to bring the toroidal field up to 11.75 T. As in the conventional case, the time-change of the current in the EQ-PFCs also contributes to the plasma current rise in this initial phase. In the following time interval $[3.65, 14.75]$ s the toroidal field reaches its flat-top value of 13 T, maintaining the plasma current. From this time on, the latter action is performed by the conventional CS, with a decrease of the total coil current from $+25.075$ to -21.300 MA. The available current swing terminates at 95 s, when the current ramp-down phase begins. The time duration of the flat-top phase is $\sim$91 s, to be compared with the 4 s in the conventional case (see figure 13). The flat-top duration is extended by a factor 22.75, a result that compares very well with the crude estimate calculated in section 4.2. We end this study with two observations. First, in this scenario the induction action of the two CSs never occurs simultaneously. Second, we had to extrapolate the time evolution of the currents in the equilibrium PF coils from the end of the flat-top of a conventional pulse ($t = 7.65$) till the end of the extended discharge. We have adopted the solution of keeping the currents constant in the equilibrium PF coils during this interval of time.

4.2.2. Scenario B. The analysis of Scenario A showed that not all the available current swing in the TFCs is needed to induce the final value of the plasma current, and provided a theoretical upper bound of the flat-top duration of the discharge when both CSs are employed. A more realistic scenario is considered in the present section, suggested by the observation that having a certain amount of toroidal field already established before the start of the plasma current ramp-up might be convenient, or even required, from an operational point of view. In Scenario B we therefore initially set up a toroidal field of 4 T, and consider this instant of time as the initial time of the discharge. The toroidal field is then increased up to its flat-top value of 13 T while the conventional CS initiates its discharging phase, contributing to plasma current induction. The plasma current and the toroidal field reach their maximum value at $t = 3.65$ s. At this time the current flowing in the TFCs remains constant till the end of the flat-top, while the conventional CS sustains the plasma current during the flat-top phase. The plasma current ramp-down begins at 70 s. This operative scenario is illustrated in figure 16. Since in this scenario the induction power associated with the rise of the toroidal field from 0 to 4 T has been 'wasted', the flat-top phase is shorter that in Scenario A, and equal to 66.35 s. We observe that in Scenario B, the two CSs act together for a certain period of the discharge, and the effect of their mutual inductance on voltage requirements should be considered.

5. Summary and conclusions

The present work deals with the potential advantages introduced by some form of tilting of the TFCs of a tokamak. Most of the literature has focused on the force reduction benefit

associated with the tilting. Here, equal attention is paid to the additional effect of poloidal magnetic flux generation and the consequent ability to contribute to plasma current induction. A fundamental difference between the conventional CS and the one associated with the TFCs tilting, is that in the latter case the plasma current induction can occur only in conjunction with a time variation of the toroidal magnetic field, and this constraint must be taken into account when envisaging operational scenarios.

The results presented in this work refer to compact high-field tokamaks, such as Ignitor or SPARC, because the problem of EM forces and of limited discharge time is exacerbated in these devices. In particular, for our study we refer to the Ignitor project, a tokamak device with minor and major radius equal to 0.47 and 1.32 m, respectively, and maximum values of plasma current and toroidal field equal to 11 MA and 13 T. The advantages associated with the tilting of the TFCs should, however, subsist also in larger devices, such as ITER. As the main plasma parameters are very different from those of compact high-field machines, however, the conclusions on force reduction and time-extension of the discharge obtainable with a synergic action of the conventional CS, and the additional one associated with the tilted TFCs, may vary significantly from the one presented in this work.

Considering only the magnetic field created by the TFCs and not by the PF coils system and the plasma current, we have quantified the maximum reduction of the total EM force acting on TFCs with their inner region tilted. A negative consequence of the tilting, however, is the insurgence of out-of-plane forces, which are, however, of smaller magnitude compared with the planar forces, and easier to cope with through bucking and wedging solutions. We observe that the tilting optimization could be activated on any region of the coil profile, and not only on the inner region as we have chosen to do in the present work, and/or it could be pursued with a goal different from the minimization of the total force. In particular, it might be convenient to perform the optimization not with the goal of minimizing the total force, but to reduce as much as possible its vertical component, and accepting the consequent amount of radial component. This solution would allow the tokamak device to take some advantage of the 'bucking' solution between the TFCs system and the conventional CS, so to facilitate the mechanical design of the device.

A consequence of the tilting which bears, in our opinion, at least an equal importance as that associated to force reduction, is that the burden of the ramp-up phase of the plasma discharge can be taken, totally or in part, by the poloidal flux produced by the tilted TFCs during the rise of the toroidal field. Using a simple circuital modeling to compute the time evolution of the total plasma current, disregarding the bootstrap current contribution as well as any noninductive current drive system, we have found that the rising of the toroidal field from 0 to 13 T produces a flux linkage that is more than sufficient to induce the flat-top plasma current of 11 MA. We have therefore presented two possible operational scenarios. In the first one (Scenario A), the maximum value of the plasma current is obtained by increasing the toroidal field from 0 to 11.75 T. The subsequent increase of the toroidal field up to 13 T is then used to maintain the plasma current in the first part of the flat-top. Once the toroidal field has reached its maximum value, the burden of maintaining the plasma current is left to the flux swing created by the conventional CS. This scenario shows that the flat-top phase, which is calculated to be of about 4 s in the reference Ignitor discharge, can be extended by a factor of $\sim$23. This value represents a theoretical upper bound of the extension time factor, since the plasma current ramp-up begins when the toroidal field is still very small. In a second operational scenario (Scenario B), the toroidal field is raised to 4 T before initiating plasma current induction. The latter is ramped up by the synergic action of the conventional solenoid and the additional one created by the TFCs tilting. The flat-top plasma current is then maintained exclusively by the conventional CS. In this scenario, the flat-top phase has been extended by a factor of $\sim$16. We notice that in the ramp-up phase the two solenoids work together to induce the loop voltage, and the mutual induction between the two solenoids should be considered. Moreover we observe that in both scenarios the heating of Cu-based TFCs would prevent such a long discharge time, and superconductor (or hybrid) coils must be employed. The latter constrain the rate of current increase, and this effect might modify the conclusions presented in this paper.

The results on the time-extension of the plasma discharge have been obtained by numerically solving a simple circuital equation for the plasma current rise. The main limitation inherent in this approach resides in the imposition as inputs of the time-evolution of the basic plasma quantities and radial profiles, such as plasma size, current density profile, and particle density and temperature profiles. Moreover, the coils contributing to current induction have been approximated with infinitely thin line conductors, and this raises questions regarding the ability of our model to reproduce the correct flux generated by the tilted TFCs. Our results must therefore be considered as approximate, and aimed only at providing a first indication on the potential benefit of TFC tilting. Moreover, no attempt has been made to verify whether the modified coils would have a negative impact on plasma equilibrium and stability, in particular during the envisaged parallel rise of the toroidal field and the plasma current. A comprehensive study, based on the 1.5D transport code coupled with an equilibrium and stability solver, must be pursued before a definitive conclusion on the advantages, or even the feasibility, of the kind of TFC tilting proposed in this work can be drawn. Finally, no attention has been paid to the actual buildability of a tilted TFCs system of the kind proposed in the present work.

The link between the rise of the toroidal magnetic field at the beginning of a discharge, and a time-varying flux linked to the plasma, might be considered to be a limiting factor for an experimental device, the goal of which is, by nature, that of exploring different operational scenarios and in particular various kinds of ramp-up procedure. On the contrary, we do not foresee limitations of this kind in a power reactor, the goal of which is to set up a reference discharge characterized by well-defined plasma parameters (current, toroidal field) and keep them unchanged during steady-state operation.

Acknowledgments

The authors affiliated with Sapienza University of Rome thank their Institution for supporting this work with the research Grant No. RP11916B86549501. The authors thank Giuseppe Ramogida for kindly providing his insight on the issue of tokamak operational scenarios, and his calculation on Ignitor plasmas.

ORCID iD

V.K. Zotta https://orcid.org/0000-0002-3518-5178

References

[1] Jong C.T.J., Mitchell N. and Sborchia C. 2011 *Fusion Eng. Des.* **58–59** 165
[2] Biancolini M.E. *et al* 2018 *IEEE Trans. Appl. Supercond.* **28** 4901405
[3] Segal D.J., Cerfon A.J. and Freidberg J.P. 2021 *Nucl. Fusion* **61** 045001
[4] Breschi M., Cavallucci L., Tronza V., Mitchell N., Bruzzone P. and Sedlak K. 2021 *Supercond. Sci. Technol.* **34** 085021
[5] Sestero A. and Briguglio S. 1988 *Fusion Eng. Des.* **6** 281
[6] Coppi B. and Lanzavecchia L. (The Ignitor Design Group) 1987 *Comments Plasma Phys. Control. Fusion* **11** 47
[7] Miura Y., Sakota M. and Shimada R. 1994 *IEEE Trans. Magn.* **30** 2573
[8] Kondoh J., Fujii K., Nomoto K., Harada T., Tsuji-Iio S. and Shimada R. 1998 *Fusion Eng. Des.* **42** 417
[9] Murakami T., Komatsu Y., Tsutsui H., Tsuji-iio S., Shimada R., Murase S. and Shimamoto S. 2000 *Fusion Eng. Des.* **51–52** 1059
[10] Tsutsui H., Nakayama K., Ito T., Ajikawa H., Nomura S., Tsuji-Iio S. and Shimada R. 2004 *Nucl. Fusion* **44** 954
[11] Habuchi T., Tsutsui H., Tsuji-Iio S. and Shimada R. 2011 *Plasma Fusion Res.* **6** 2405150
[12] Clark A.W., Doumet M., Hammond K.C., Kornbluth Y., Spong D.A., Sweeney R. and Volpe F.A. 2014 *Fusion Eng. Des.* **89** 2732
[13] Bombarda F. and Gatto R. 2015 ENEA Technical Report 14/529 (Frascati: ENEA CR)
[14] Gatto R. and Bombarda F. 2019 *Fusion Eng. Des.* **147** 111232
[15] Stober J. *et al* 2011 *Nucl. Fusion* **51** 083031
[16] Granucci G. 2015 *Nucl. Fusion* **55** 093025
[17] Ambrosino R. *et al* 2021 *Fusion Eng. Des.* **167** 112330
[18] Granucci G. 2018 *45th EPS Conf. on Plasma Physics (Prague, Czech Republic, 2–6 July 2018)* p 4.1071
[19] Bucalossi J. *et al* 2009 *Proc. 15th Joint Workshop on Electron Cyclotron Emission and Electron Cyclotron Resonance Heating (EC-15)* (*Yosemite National Park, CA, USA, 10–13 March 2008*) (https://doi.org/10.1142/6859)
[20] Jackson G.L., Austin M.E., deGRASSIE J.S., Hyatt A.W., Lohr J.M., Luce T.C., Prater R. and West W.P. 2010 *Fusion Sci. Technol.* **57** 27
[21] Bae Y.S. *et al* 2009 *Nucl. Fusion* **49** 022001
[22] Ricci D. *et al* 2019 *46th EPS Conf. on Plasma Physics (Milan, 8–12 July 2019)* (available at: http://ocs.ciemat.es/EPS2019PAP/pdf/O5.103.pdf)
[23] Sinha J. *et al* 2022 *Nucl. Fusion* **62** 066013
[24] Coppi B (the Ignitor Project Group) 1996 *Ignitor Program General Report* MIT-RLE Report PTP 96/03 (Cambridge, MA: Massachusetts Institute of Technology)
[25] Coppi B., Nassi M. and Sugiyama L.E. 1992 *Phys. Scr.* **45** 112
[26] Greenwald M. *et al* 2018 The high-field path to practical fusion energy *Technical Report* PSFC/RR-18-2 (Plasma Science and Fusion Center, MIT)
[27] Wolfram Research, Inc. 2021 *Mathematica, Version 12.3.0* (Champaign, IL: Wolfram Research)
[28] Creely A.J. *et al* 2020 *J. Plasma Phys.* **86** 865860502
[29] Coppi B. *et al* 2015 *Nucl. Fusion* **55** 053011
[30] Ramogida G. (The Ignitor Engineering Workgroup) 2007 *1st Ignitor Meeting ENEA (Frascati, 18 January 2007)*
[31] Cenacchi G. and Taroni A. 1988 JETTO: a free-boundary plasma transport code (basic version) *Report* JET-IR(88)03 (Abingdon: JET Joint Undertaking)
[32] Ramogida G. and Roccella M. (the Ignitor Engineering Workgroup) 2004 Engineering of the Ignitor machine Workshop "Ignitor", University of Pisa, Italy
[33] Freidberg J.P. 2007 *Plasma Physics and Fusion Energy* (Cambridge: Cambridge University Press)
[34] Hirshman S.P. and Neilson G.H. 1986 *Phys. Fluids* **29** 790